

Numerical Modelization for Equilibrium Position of a Static Loaded Hydrodynamic Bearing

Mô phỏng số vị trí cân bằng cho ổ đỡ thủy động dưới tác dụng của tải trọng tĩnh

Le Anh Dung, Tran Thi Thanh Hai, Luu Trong Thuan*

Hanoi University of Science and Technology - No. 1, Dai Co Viet Str., Hai Ba Trung, Ha Noi, Viet Nam

Received: October 24, 2019; Accepted: March 20, 2020

Abstract

This paper presents a numerical simulation of hydrodynamic journal bearing lubrication by using finite element method to solve Reynolds equation in static load condition. Reynolds boundary condition is applied in this research in order to yield oil film pressure distribution at a given oil supply hole position. When the pressure distribution is obtained, the equilibrium position of the housing bearing can be determined by using Newton-Raphson method applied on the equilibrium equation of the charge. The equilibrium positions are simulated in different parameters of the journal speed and the applied load. The results show that at the different sections of bearing, the starting disruption positions are different and the middle section along the axial direction shows the maximum pressure and gradually decreases toward two ends of bearing. On the other hand, the more loads applied, the distance from the calculated equilibrium position to the journal center gets farther. The faster journal rotation speed makes the balance point closer to the journal center.

Keywords: Hydrodynamic journal bearing, Cavitation, Equilibrium position, Reynold boundary condition, Static load.

Tóm tắt

Bài báo này đưa ra mô phỏng số cho bôi trơn ổ đỡ thủy động bằng cách sử dụng phương pháp phần tử hữu hạn để giải phương trình Reynolds ở chế độ tải tĩnh. Áp dụng điều kiện biên Reynolds để giải ra phân bố áp suất màng dầu. Sau đó xác định vị trí cân bằng của bạc bằng cách giải phương trình cân bằng tải sử dụng thuật giải Newton-Raphson. Vị trí cân bằng được mô phỏng ở các giá trị khác nhau về tốc độ quay của trục và tải tác dụng. Kết quả cho thấy ở các mặt cắt khác nhau của ổ theo phương dọc trục, vị trí bắt đầu gián đoạn là khác nhau, mặt cắt giữa ổ đạt giá trị áp suất lớn nhất và giảm dần về hai phía của ổ theo phương dọc trục. Khi tải càng lớn vị trí tâm bạc càng cách xa tâm trục. Tốc độ quay của trục càng lớn thì vị trí cân bằng càng gần với tâm trục.

Từ khóa: Ổ đỡ thủy động, Gián đoạn màng dầu, Vị trí cân bằng, Điều kiện biên Reynolds, Tải trọng tĩnh.

1. Introduction

Widely used in rotary machineries, hydrodynamic journal bearings allow for the large load operation at the average rate of rotation. Hydrodynamic journal bearing based on hydrodynamic lubrication, which can be described as the load-carrying surfaces of the bearing are absolutely separated by a thin film of lubricant in order to prevent metal-to-metal contact.

The equation governing the pressure generated in the lubricant film was first derived by Reynolds [1]. In 1962, Dowson [2] generalized the Reynolds equation considering the variation of fluid properties both across and along the fluid film thickness. In 1930s, Swift [3] và Stieber [4] presented the Swift-Stieber boundary condition (so-call Reynolds

boundary) to study the pressure distribution at steady-state. Hence the Reynolds equation solves using numerical technique [5] with help of computer program. In 1989, Chen and Chen [6] studied the steady-state characteristics of finite bearings including inertia effect using the Reynolds expansion formulation of Banerjee et al [7]. In 1991, Pai and Majumdar [8] analyzed the stability characteristics of submerged plain journal bearings under a unidirectional constant load and variable rotating load. In 1999, Raghunandana and Majumdar [9] analyzed the effects of non-Newtonian lubricant on the stability of oil film journal bearings under a unidirectional constant load. In 2000, Kakoty and Majumdar [10] analyzed the stability of journal bearings under the effects of fluid Inertia, the next year, Jack and Stephen [11] reviewed the theory of finite element applied on elasto-hydrodynamic lubrication. In 2016, Biswas, Chakraborti and Saha [12] performed the experiments to study the stability of three lobe journal bearing.

* Corresponding author: Tel.: (+84) 978263926
Email: hai.tranthithanh@hust.edu.vn

This research tends to study the stability of the hydrodynamic journal bearing, takes account of cavitation presented by Reynold boundary condition. Finite element method (FEM) were used for modeling finite journal bearing combined with Newton-Raphson iteration to calculate the equilibrium position of the static loaded bearing.

2. Analytical method and algorithm

2.1. Reynold equation and Cavitation modeling

The Reynold differential equation [2] was written as, assuming the fluid is incompressible and in a steady state condition:

$$L(p) = b \quad (1)$$

$$\begin{cases} L(\cdot) = \frac{\partial}{\partial x} \left(h^3 \frac{\partial \cdot}{\partial x} \right) + \frac{\partial}{\partial z} \left(h^3 \frac{\partial \cdot}{\partial z} \right) \\ b = 6\mu U \frac{\partial h}{\partial x} \end{cases} \quad (2)$$

where p is pressure distribution vector, h is the film thickness, U is the journal speed, μ is the dynamic viscosity.

Cavitation is taken into account when solving Equation (1) (Eq. 1) within Reynolds boundary condition. In the expansion of the oil film included the active zone and the cavitation zone showed in Fig.1:

- The active zone Ω^+ : $p \geq 0$, the surface of shaft and housing bearing is absolutely separated by the lubrication oil film.
- The cavitation zone Ω^0 : $p = 0$, where interlace with vapor bubbles.

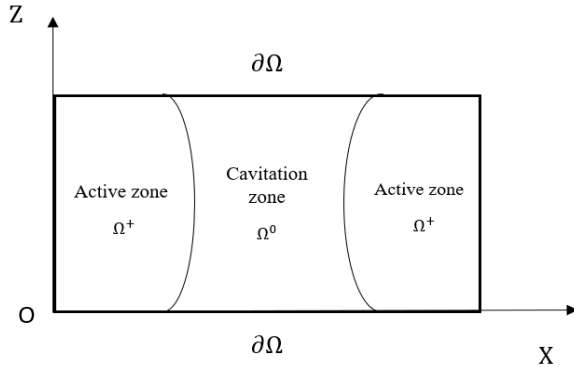


Fig. 1. The expansion of oil film in journal bearing.

The film thickness is described as:

$$h = C(1 + \varepsilon_x \cos \theta + \varepsilon_y \sin \theta) \quad (3)$$

where $\theta = \frac{x}{R}$, C is the radial clearance. $\varepsilon_x, \varepsilon_y$ is the dimensionless equilibrium position.

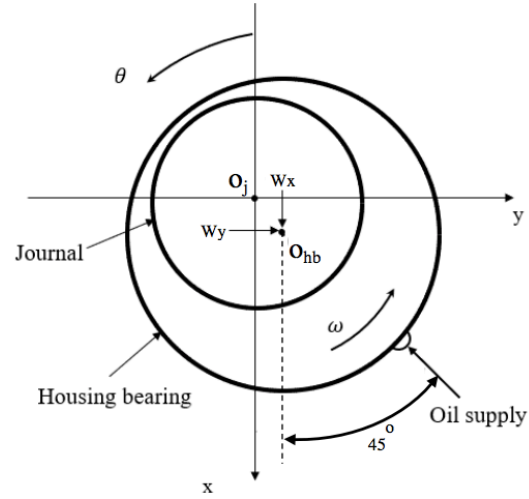


Fig. 2. Geometry of the journal bearing.

Within a Sobolev space $H_0^1(\Omega^+)$ and $K = \{p \in H_0^1(\Omega^+); p \geq 0 \text{ in } \Omega^+\}$ is a subset of the Sobolev space; in $H_0^1(\Omega^+) \times H_0^1(\Omega^+)$ by using a symmetric and bilinear form as:

$$a(\cdot, \cdot) = \iint \frac{\partial}{\partial x} \left(h^3 \frac{\partial \cdot}{\partial x} \right) + \frac{\partial}{\partial z} \left(h^3 \frac{\partial \cdot}{\partial z} \right) dXdZ \quad (4)$$

And a linear function in $H_0^1(\Omega^+)$:

$$b(\cdot) = \iint b(\cdot) dXdZ \quad (5)$$

Above equation can be express as an inequality which is to find a function $p \in K$ and $p \geq 0$ satisfied:

$$a(p, q) \geq b(q) \quad (6)$$

By using finite element method, p and q can be expressed as:

$$\begin{aligned} p &= \sum_{i=1}^n p_i N_i = \tilde{p} \cdot N \\ q &= \sum_{i=1}^n q_i N_i = \tilde{q} \cdot N \end{aligned} \quad (7)$$

where n is the total number of mesh points, N is the global polynomials function vector.

Substitute (7) into (6) yields: find $p \geq 0$ that

$$\forall \tilde{q} \geq 0, \tilde{q}^T A \tilde{p} \geq \tilde{q}^T \tilde{b} \quad (8)$$

where $A = [a_{ij}]$ is the “stiffness matrix” and $\tilde{b} = [b_i]$ is the “load vector”. Here so a_{ij} and b_i can be taken by substituting N_i and N_j into Eq. (4) and Eq. (5):

$$a_{ij} = a(N_i, N_j); \tilde{b}_i = b(N_i) \quad (9)$$

The discrete inequality is equivalent to the linear equations: find $\tilde{p}, \tilde{q} \geq 0$ such that:

$$\begin{cases} A \tilde{p} - \tilde{b} = \tilde{q} \\ \tilde{q}^T \tilde{p} = 0 \end{cases} \quad (10)$$

For all mesh points $I_n = \{1, 2, \dots, n\} = I_a \cup I_b$ where:

$$\begin{cases} \forall i \in I_a, p_i \geq 0 \text{ và } q_i = 0 \\ \forall i \in I_b, p_i = 0 \text{ và } q_i \geq 0 \end{cases} \quad (11)$$

I_a is the number of mesh points in active zone, I_b is the number of mesh points in cavitation zone and the boundary zone including the oil supply elements. Eq. (10) can be rewritten as:

$$\begin{bmatrix} A_{aa} & A_{ab} \\ A_{ba} & A_{bb} \end{bmatrix} \begin{Bmatrix} \tilde{p}_a \\ 0 \end{Bmatrix} - \begin{Bmatrix} \tilde{b}_a \\ \tilde{b}_b \end{Bmatrix} = \begin{Bmatrix} 0 \\ \tilde{q}_b \end{Bmatrix} \quad (12)$$

Eq. (12) can be rewritten as:

$$\begin{cases} \hat{A}\tilde{p} = \hat{b} \\ \tilde{q} = A\tilde{p} - \tilde{b} \end{cases} \quad (13)$$

where

$$\hat{A} = [\hat{a}_{ij}] = \begin{bmatrix} A_{aa} & 0 \\ 0 & I \end{bmatrix}, \hat{b} = \{\hat{b}_i\} = \begin{Bmatrix} \tilde{b}_a \\ 0 \end{Bmatrix} \quad (14)$$

\hat{a}_{ij}, \hat{b}_i is determined as follow

$$\begin{cases} \hat{a}_{ij} = a_{ij} \text{ if } i, j \in I_a; \hat{b}_i = \tilde{b}_i \text{ if } i \in I_a \\ \hat{a}_{ij} = 1; \hat{b}_i = 0 \text{ if } i \in I_b \\ \hat{a}_{ij} = 0 \text{ if } i \in I_a, j \in I_b \text{ if } i \in I_b, j \in I_a \end{cases} \quad (15)$$

2.2. Oil film force and equilibrium equation

Once pressure distribution vector p is determined, oil film force can be evaluated as:

$$f(x, y) = \begin{Bmatrix} f_x \\ f_y \end{Bmatrix} = \begin{Bmatrix} -\iint_{\Omega} p \cos \theta dXdZ \\ -\iint_{\Omega} p \sin \theta dXdZ \end{Bmatrix} \quad (16)$$

Substitute the expression of p (7) to above Eq.(16):

$$f(x, y) = \begin{Bmatrix} f_x \\ f_y \end{Bmatrix} = \begin{Bmatrix} -\tilde{p} \iint_{\Omega} N \cos \theta dXdZ \\ -\tilde{p} \iint_{\Omega} N \sin \theta dXdZ \end{Bmatrix} \quad (17)$$

Let the two constant vectors:

$$S = \iint_{\Omega} N \cos \theta dxdz \quad R = \iint_{\Omega} N \sin \theta dXdZ \quad (18)$$

Then Eq. (17) becomes:

$$F_x = -S^t \tilde{p} \quad F_y = -R^t \tilde{p} \quad (19)$$

The Jacobian matrix of the oil film force related to the equilibrium position

$$J_u[f(x, y)] = \begin{bmatrix} \frac{\partial F_x(x, y)}{\partial x} & \frac{\partial F_x(x, y)}{\partial y} \\ \frac{\partial F_y(x, y)}{\partial x} & \frac{\partial F_y(x, y)}{\partial y} \end{bmatrix} \quad (20)$$

Substitute Eq. (19) into Eq. (20) gives:

$$J_u[f(x, y)] = -\begin{Bmatrix} S^t \\ R^t \end{Bmatrix} [\tilde{p}_x \quad \tilde{p}_y] = -\begin{bmatrix} S^t \tilde{p}_x & S^t \tilde{p}_y \\ R^t \tilde{p}_x & R^t \tilde{p}_y \end{bmatrix} \quad (21)$$

where $\tilde{p}_x = \frac{\partial \tilde{p}}{\partial x}, \tilde{p}_y = \frac{\partial \tilde{p}}{\partial y}$.

The first of Eq. (13) can be rewritten as:

$$\hat{A}(x, y) \cdot p = \hat{b}(x, y) \quad (22)$$

Taking partial differentiation of above Eq. (22) with respected to x, y yield:

$$\hat{A} \cdot [\tilde{p}_x, \tilde{p}_y] = [-\hat{A}_x \cdot p + \hat{b}_x, -\hat{A}_y \cdot p + \hat{b}_y] \quad (23)$$

where $\hat{A}_x = \frac{\partial \hat{A}}{\partial x}, \hat{A}_y = \frac{\partial \hat{A}}{\partial y}, \hat{b}_x = \frac{\partial \hat{b}}{\partial x}, \hat{b}_y = \frac{\partial \hat{b}}{\partial y}$.

The stiffness components $\hat{A}_x = [\hat{a}_{ij,x}], \hat{A}_y = [\hat{a}_{ij,y}]$,

$\hat{b}_x = [\hat{b}_{i,x}], \hat{b}_y = [\hat{b}_{i,y}]$ is determined as:

$$\begin{cases} \hat{a}_{ij,k} = \frac{\partial a_{ij}}{\partial k} (k = x, y) \text{ if } i, j \in I_a \\ \hat{b}_{i,k} = \frac{\partial b_i}{\partial k} (k = x, y) \text{ if } i \in I_a \\ \hat{a}_{ij,k} = 0 (k = x, y), \hat{b}_{i,k} = 0 (k = x, y) \text{ else} \end{cases} \quad (24)$$

Substitute (9) into (4) and (5) then taking partial derivatives with respect to x and y yields:

$$\begin{aligned} \frac{\partial a_{ij}}{\partial x} &= \iint_{\Omega} 3h^2 \cos \theta \left[\frac{\partial}{\partial x} \left(h^3 \frac{\partial p}{\partial x} \right) + \frac{\partial}{\partial z} \left(h^3 \frac{\partial p}{\partial z} \right) \right] dXdZ \\ \frac{\partial a_{ij}}{\partial y} &= \iint_{\Omega} 3h^2 \sin \theta \left[\frac{\partial}{\partial x} \left(h^3 \frac{\partial p}{\partial x} \right) + \frac{\partial}{\partial z} \left(h^3 \frac{\partial p}{\partial z} \right) \right] dXdZ \end{aligned} \quad (25)$$

$$B_x = \iint_{\Omega} N \sin \theta dXdZ \quad B_y = \iint_{\Omega} N \cos \theta dXdZ \quad (26)$$

Thus, when those components (25) (26) was calculated and p is obtained from (13), Eq. (22) can be readily solved by using Newton-Raphson iterative method. The load is put on housing and can be denoted as $w = [W_x, W_y]^t$ and the dimensionless equilibrium position is supposed to be $u_0 = [\varepsilon_x^0, \varepsilon_y^0]^t$, and the oil film force $f(x, y) = f(C, u)$.

The equilibrium equation is as follow:

$$F(C, u_0) - w = 0 \quad (27)$$

In order to solve the nonlinear equation, Newton- Raphson method is commonly used due to its rapidly convergence and highly accurate approximation. So, the difficulty left is to determine the Jacobian matrix which is described at Eq. (21). Let u^0 be the initial value of the equilibrium position, u^k be the value of iterative step k . Thus, the iterative process is given by:

$$u^{k+1} = u^k - J_u(f(C, u^k)) \cdot [F(C, u^k) - w] \quad (28)$$

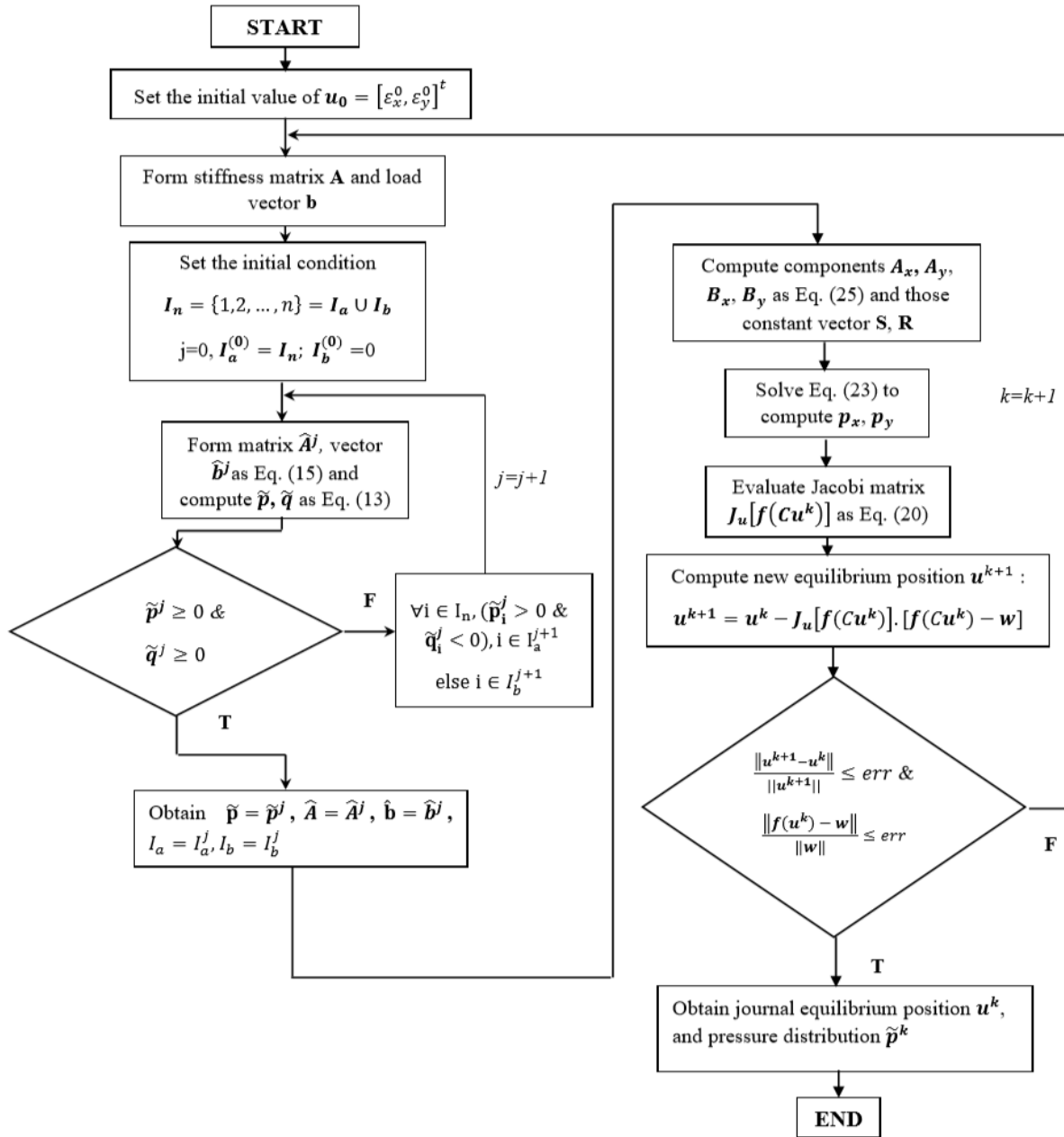


Fig. 3. Algorithm diagram

This iteration process ends when the following error bound condition *err* is satisfied:

$$\frac{\|u^{k+1} - u^k\|}{\|u^{k+1}\|} \leq err \quad \& \quad \frac{\|f(u^k) - w\|}{\|w\|} \leq err$$

In this paper, $err = 10^{-5}$ is applied, the closer value of *err* to zero gives the more accurate results but causes more iterative steps

The Fig.3 fully describes the programming algorithm for the numerical simulation.

3.Simulation results

The bearing expansion surface is divided into 4-node quadrilateral element mesh. The program was built on the MATLAB 2015a and applied to the specific bearing described in Table-1. The oil supply hole is at showed in Fig. 2 and at the center section of the bearing along axial direction.

Fig.4 illustrates the pressure distribution of the bearing at $w = [W_x, W_y]^t = [140, 0]$ N and 300 rpm of journal speed. The pressure distribution contains

two regions: the active and the cavitation area. The former has the pressure change in both axial and circumference directions, otherwise, the pressure remains constant in the latter area. The cavitation area starts from about 80° to 238.5° in circumference direction. Pressure distribution is symmetric and decreases more and more along the middle section toward two ends of the bearing.

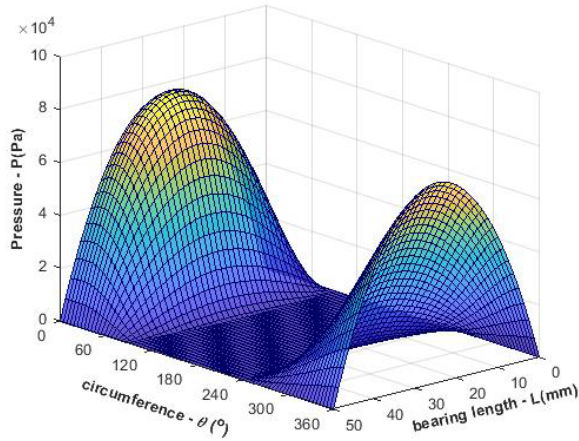


Fig. 4. Pressure distribution of journal bearing $w = [W_x, W_y]^t = [140, 0]$ N and 300 rpm of journal speed

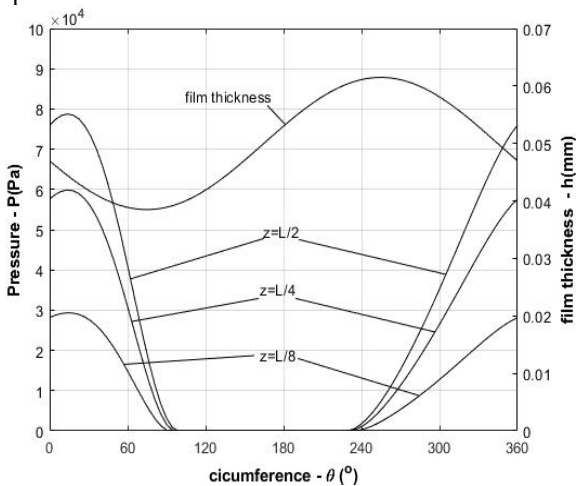


Fig. 5. Pressure distribution and film thickness of different sections along the axial direction.

Table 1. The parameter of journal bearing

Bearing specification	Value	Unit
Journal diameter (D)	70	mm
Bearing length (L)	50	mm
Axial clearance (C)	0.05	mm
Lubricant viscosity (μ)	0.015	Pa.s
Oil supply hole diameter (D_s)	5	mm

Fig.5 illustrates the pressure distribution and the film thickness of the different sections at the circumference direction. In different sections of the bearing, the starting and the ending position of the cavitation is slightly different, the lowest cavitation range occurs at the middle section $z=L/2$ (from 99° to 225°) and increases toward two ends of the bearing $z=0$ (from 80° to 238.5°). The high pressure zone occurs where the film thickness is about to decrease and the max pressure position is close to the minimum oil film thickness. Thus, the film thickness is compatible with the oil pressure in load-bearing area.

So as to study the stability of the journal bearing at different parameters, by sequentially modifying the applied load and the journal speed, the change of equilibrium position is showed in Fig. 6 and Fig. 7.

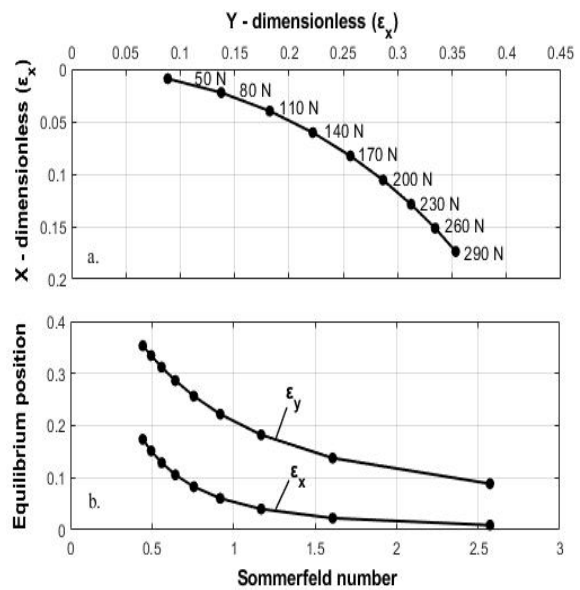


Fig. 6. Dimensionless equilibrium position at 300 rpm of journal speed respect to applied loads and Sommerfeld numbers

Fig.6a shows that the more loads applied, the distance from the equilibrium of housing bearing position to the journal center (0,0) gets farther. However, for each 30 N of the load increase, the distance between the next balance point and the previous point tends to decrease. It is reasonable since these oil film forces are nonlinear function of the housing bearing center [13].

As another expression with respecting to Sommerfeld number $S = \frac{\mu LD}{W} \left(\frac{R}{C}\right)^2$ in Fig.6b, similarly, the values of ϵ_x and ϵ_y decrease when the Sommerfeld number increases. At the lowest Sommerfeld number, ϵ_y is about two times larger than ϵ_x . Otherwise at the highest one, ϵ_x is very close

to zero, which means within the increase of the Sommerfeld number values, as the decrease of load, the equilibrium position moves closer to the y-axis. Because the static load in this research is respect to x direction, when the load decreases the equilibrium position changes along x axis more than y axis.

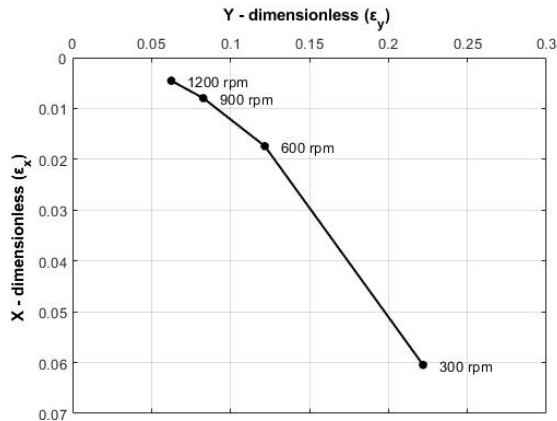


Fig. 7. Dimensionless equilibrium position with different speeds of journal at 140 N of applied load

Fig.7 shows that the rise of the journal speed causes the equilibrium point changes significantly, get closer and closer to the journal center. This leads to the descending of the maximum film thickness and the ascending of the minimum film thickness which usually causes the load-bearing zone to spread. Thus, the higher speed gives the better effects of the hydrodynamic lubrication, however, in reality the speed depends on the specific demands of the machine.

4. Conclusion

This research numerically simulates the equilibrium position of the journal bearing by using finite element method to solve Reynold equation in static load condition. Cavitation is taken into account which is related to the specification of Reynold boundary condition.

As the result, at the different sections of bearing, the starting disruption positions are different, the middle section along the axial direction shows the maximum pressure and gradually decreases toward two ends of bearing. On the other hand, the more loads applied, the distance from the calculated equilibrium position to the journal center gets farther. Within the increase of the Sommerfeld number values, the equilibrium position moves closer to the y-axis.

When journal rotation speed increases, the balance point gets closer to the journal center.

The result of this research is the foundation for the dynamic loaded bearing studies.

References

- [1] Reynolds, On the theory of lubrication and its application to Mr. Beauchamp Tower's experiment, Phil. Trans. R. Sot. London, 177 (1886) 157.
- [2] Dowson D., A Generalized Reynolds Equation for Fluid-Film Lubrication, Elsevier publication, IJMSPL. Vol. 4 (1962) pp. 159-170.
- [3] Swift, H. W., The Stability of Lubricating Films in Journal Bearings, Proc.-Inst. Civ. Eng., 233, (1932) 267-288.
- [4] Stieber W., Das Schwimmlager, Verein Deuqtscher Ingenieure, Berlin (1993).
- [5] Vohr J. H., Numerical Methods in Hydro-dynamic Lubrication, CRC Handbook of Lubrication Vol. 2 (1983) 93-104.
- [6] Chen, Chen-Hain, and Chen, Chato-Kuang, The Influence of Fluid Inertia on the Operating Characteristics of Finite Journal Bearings, Wear, 131 (1989) 229-240.
- [7] Banerjee, M. B., Shandil, R. G., Katyal, S. P., Dube, G. S., Pal, T. S., and Banerjee, K., 1986, A Nonlinear Theory of Hydrodynamic Lubrication, J. Math. Anal. Appl., 117, (1986) 48-56.
- [8] Pai, R. and B.C. Majumdar, Stability analysis of flexible supported rough submerged oil journal bearings. Tribol. T., 40(3) (1991) 437-444.
- [9] Raghunandana, K., and Majumdar, B. C., Stability of Journal Bearing Systems Using Non-Newtonian Lubricants: A Non-Linear Transient Analysis, Tribol. Int., 32, (1999) pp. 179-184.
- [10] Kakoty, S.K. and B.C. Majumdar. Effect of fluid inertia on stability of oil journal bearings. ASME J. Tribol., 122 (2000) 741-745.
- [11] Jack,F.B., Stephen B. Finite element analysis of elastic engine bearing lubrication: theory (2001).
- [12] Biswas, N., Chakraborti, P., Saha, A., & Biswas, S. Performance & stability analysis of a three-lobe journal bearing with varying parameters: Experiments and analysis (2016).
- [13] Frêne Jean, Daniel Nicolas, Bernard Degueurce, Daniel Berthe, Maurice Godet, Préfacede Gilbert Riollet., Paris 1990, Lubrification hydrodinamique Paliers et butées, 151-163